Anatomy Relationship around Internal Carotid Artery in the Endoscopic Surgery of Nasopharynx: A Study Based on Computed Tomography Angiography

Zhen Gao[1] Fang-lu Chi[1]

[1] Department of Otology and Skull Base Surgery, Eye and ENT Hospital, Fudan University, Shanghai, China

Address for correspondence Fang-lu Chi, MD, PhD, No. 83, Fenyang Road, Shanghai 200031, China (e-mail: chifanglu@126.com).

J Neurol Surg B 2015;76:176–182.

Abstract

Objective Anatomic knowledge is needed to avoid injury to internal carotid artery (ICA) during the endoscopic surgery around nasopharynx and its surrounding space.

Design We prospectively studied the computed tomography angiography (CTA) data of 28 patients with image processing software. Special attention was given to ICA and various landmarks around nasopharynx.

Results The anatomic relationship between ICA and different landmarks around nasopharynx was clearly presented in three-dimension. The fossa of Rosenmuller is the nearest point of the nasopharyngeal cavity to ICA. The opening of the Vidian canal in the middle cranial fossa could be either above, below, or at the level of the horizontal segment of petrous ICA. The pharyngeal trunk of the ascending pharyngeal artery can also be clearly identified in most reconstructed CTA images. Multiple anatomic relationships were also quantified.

Conclusions Reconstructed CTA can provide key anatomic information for a safe and accurate endoscopic dissection around nasopharynx.

Keywords
- nasopharynx
- internal carotid artery
- Vidian canal
- computed tomography angiography
- infratemporal fossa

Introduction

The nasopharynx, which deeply positions in the center of the head is the original site of several malignancies such as rhabdomyosarcomas, melanomas, lymphomas, and especially the nasopharyngeal carcinoma (NPC), which has a high prevalence in Southern China and Southeast Asia.[1,2] It is reported that the highest incidence of NPC in China is approximately 100-fold higher than the one observed in European and North American population.[3] In addition, the nasopharynx can also be involved by malignancies arising from paranasal sinus, pterygopalatine fossa, infratemporal fossa, salivary gland, and skull base. The treatment of nasopharyngeal malignancies is a multi-discipline art.[4] Surgery plays a primary role in the treatment of malignancies with glandular or mesenchymal differentiations in the nasopharynx; and nowadays, it is more and more recommended as one of the best salvage treatments for locally recurrent NPC.[5,6]

Since Fisch first reported the infratemporal fossa approach to the nasopharynx for radical resection of T1- and T2-NPC.[7] Numerous invasive surgical approaches have been developed to handle the nasopharyngeal malignancies. The nasopharynx and its surrounding space can be reached anteriorly through the maxillary,[8] inferiorly through the oral cavity or mandibular[9–11]; or laterally through the infratemporal fossa.[7] In the past 10 years, with the development of endoscopic instruments and surgical technique, endonasal endoscopic approach to the nasopharynx has been developed to reduce the potential morbidity of an invasive surgical procedure.[12–18] Endoscopic approach has its own unique

received
December 27, 2013
accepted after revision
August 28, 2014
published online
December 24, 2014

DOI http://dx.doi.org/10.1055/s-0034-1395488.
ISSN 2193-6331.

advantages such as excellent illumination and image magnification of the surgical field. However, since the dissection space under endoscope is not adequate enough for a sufficient exposure, sometimes it is difficult to identify key surgical landmarks for a safe and accurate surgical orientation.

For the proximity of internal carotid artery (ICA), the biggest risk to perform surgery in the nasopharynx and its surrounding space is the rupture of parapharyngeal or petrous ICA which could lead to death.[18,19] To avoid injury to ICA, it is essential to understand the anatomic relationship around parapharyngeal and the petrous ICA in detail. As demonstrated before, computed tomography angiography (CTA) is a potent tool to assess anatomic information around vascular structures.[20] In the current study, we have explored the possibility of using CTA to get adequate anatomic knowledge in the nasopharynx and its surrounding space, especially around the parapharyngeal and petrous ICA. With the help of image processing software, we reconstructed ICA and various landmarks around nasopharynx in three-dimension (3D). Several key anatomic relationships have also been quantified on the multiplanar or 3D-reconstructed CTA images.

Materials and Methods

We prospectively studied the CTA data of 28 patients (56 sides). The original 0.45-mm slices DICOM data were transferred into the independent software Mimics 12.1 (Materialize HQ, Leuven, Belgium) and then processed in it. Overall, 20 patients were males and 8 were females. The patients' age ranged from 18 to 77 years, and the average age was 55.3 years. No patients had any lesions around the nasopharynx and the scanning was performed for reasons unrelated to skull base surgery. CTA was performed using Philips Brilliance iCT (Philips, Andover, Massachusetts, United States). The whole skull with 0.45-mm slices were acquired in about 10 seconds. Ultravist 300 contrast material (Bayer Schering Pharma AG, Berlin, Germany) was injected into an ulnar vein with 1-minute delay before the initiation of scanning. In Mimics, observation was performed with a contrast scale between −150 and 1,700 HU. To clearly represent the anatomic relationships in the nasopharynx and its surrounding space, especially around the parapharyngeal and petrous ICA, 3D models representing different anatomic structures were built from CTA by Mimics' volume-rendering function. These structures included the parapharyngeal and petrous ICA, the lumen of nasopharynx, the sphenoid bone, the atlas, the Eustachian tube, and part of the middle and lateral skull base. Since the lumen of Eustachian tube could not be identified on CTA, we reconstructed the two openings of the Eustachian tube as well as sulcus tubae and then connected them with straight line (►**Fig. 1A**). In this study, oblique slices across different structures were also reconstructed. Based on these slices, the following measurements were considered: The distance from the posterior margin of medial or lateral pterygoid plate to the parapharyngeal ICA; the distance from the anterior tubercle of atlas to the parapharyngeal ICA; the distance from fossa of Rosenmuller to the parapharyngeal ICA; the distance from fossa of Rosenmuller

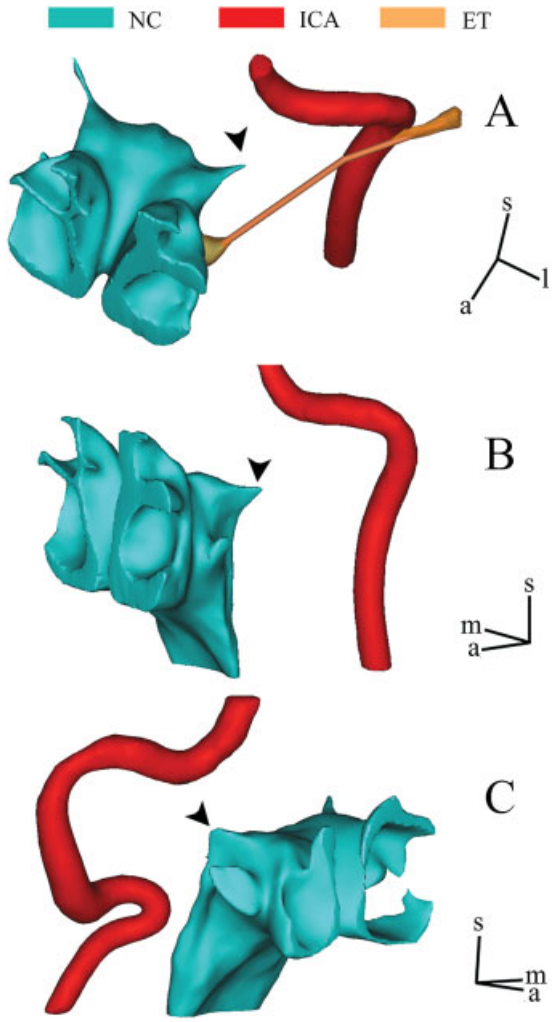

Fig. 1 3D reconstructed images of ICA, NC, and ET. The arrowhead indicates the fossa of Rosenmuller in all the panels. (A) The anatomic relationship between ICA, NC, and ET. (B) Typical anatomic relationship between ICA and the NC. The fossa of Rosenmuller is the nearest point of the whole nasopharyngeal cavity to ICA. (C) The anatomic relationship between ICA and the NC in one patient with torturous parapharyngeal ICA. The fossa of Rosenmuller is no longer the nearest point of the whole NC to ICA. 3D, three-dimension; a, anterior; ET, Eustachian tube; ICA, internal carotid artery; l, lateral; m, medial; NC, nasopharyngeal cavity; s, superior.

through the foramen lacerum to the petrous ICA; the distance from the pharyngeal tubercle of occipital bone to the parapharyngeal ICA; the distance from foramen ovale, foramen lacerum, foramen spinosum, sulcus tubae to the external aperture of petrous ICA; the length of Vidian canal; the distance between foramen rotundum and the opening of Vidian canal. We used Photoshop (Adobe Systems Incorporated, San Jose, California, United States) for processing images used for figures. The Student *t*-test was used to determine statistical significance.

Results

By 3D and multiplanar reconstruction, the anatomic relationship between nasopharyngeal cavity and ICA was first

examined and quantified. Generally, the fossa of Rosenmuller was the point of the whole nasopharyngeal cavity that had the shortest distance to both parapharyngeal and petrous ICA (►**Fig. 1B**). On the axis slices, the fossa of Rosenmuller usually directly pointed to the parapharyngeal ICA. However, such an anatomic relationship was not consistent when the parapharyngeal ICA was torturous (►**Fig. 1C**). In our study, the happen rates of torturous parapharyngeal ICA is 7.1% (4 in 56 cases). Under such condition, the nearest point from the nasopharyngeal cavity to the ICA was irregular and no longer fixed to the fossa of Rosenmuller. On multiplanar reconstruction images, the distance from the fossa of Rosenmuller to the parapharyngeal ICA was 9.14 ± 3.46 mm; while the distance from the fossa of Rosenmuller to petrous ICA through foreman lacerum was 11.21 ± 3.00 mm (►**Table 1**). No significant difference between right and left sides has been noticed.

On axis sections, several other anatomic relationships between bony landmarks of nasopharyngeal cavity and parapharyngeal ICA have also been measured. The distance from the pharyngeal tubercle of the occipital bone to the parapharyngeal ICA was 25.48 ± 3.20 mm, the distance from the anterior tubercle of atlas to the parapharyngeal ICA was 22.82 ± 3.69 mm (►**Table 1**). No significant difference between right and left sides has been noticed.

Following, the anatomic relationships between bony landmarks in pterygopalatine fossa as well as infratemporal fossa and parapharyngeal ICA have been studied in detail. On the posterior wall of the pterygopalatine fossa, the opening of Vidian canal and foramen rotundum could be identified on both 3D and multiplanar reconstructed images (►**Fig. 2A**). The distance between them was 7.75 ± 2.23 mm. The length of Vidian canal was 14.40 ± 1.93 mm (►**Table 1**). No significant difference between right and left sides has been noticed. The course of Vidian canal was from medial to lateral in 94.8% of all cases (55 in 58 cases). In the rest 5.2% samples (3 in 58 cases), the course of Vidian canal was straight. The relative position of the opening of the Vidian canal in the middle cranial fossa to petrous ICA was classified as either the opening of Vidian canal is below, above, or just at the level of the horizontal segment of petrous ICA (►**Fig. 3**). In the present study, the opening of the Vidian canal in the middle cranial fossa was below, above or at the level of the horizontal segment of petrous ICA in 79.3, 6.9, and 13.8% of all samples respectively (46, 4, and 8 in 58 cases, respectively).

In the infratemporal fossa, the parapharyngeal ICA is behind or a bit lateral to the pterygoid process in 3D image (►**Fig. 2B**). By using axis images at different levels, the distance from the posterior edge of medial and lateral pterygoid plate to the parapharyngeal ICA was measured. At the level of basis nasi, the distance from the posterior edge of the medial pterygoid plate to the parapharyngeal ICA was 26.57 ± 4.06 mm, while the distance from the posterior edge of lateral pterygoid plate to the parapharyngeal ICA was 19.71 ± 3.65 mm. At the level of Rosenmuller fossa, such distances were 26.06 ± 3.30 mm and 19.70 ± 3.20 mm, respectively (►**Table 1**). No significant difference between right and left sides has been noticed.

The ceiling of infratemporal fossa was checked from below in the 3D image. On the corresponding skull base, the foramen lacerum, the foramen ovale, the foramen spinosum, the sulcus tubae, and the external aperture of petrous ICA could be clearly identified (►**Fig. 2C**). As the main landmarks around the inlet of petrous ICA, the foramen spinosum, and the foramen ovale located roughly anterior to the external aperture of petrous ICA, and the foramen ovale was anteriormedial to the foramen spinosum. On multiplanar

Table1 Quantitative anatomic data obtain from CTA images

Measurements	*n*	Mean (mm)	SD (mm)	Min (mm)	Max (mm)
Rosenmuller fossa to parapharyngeal ICA	56	9.14	3.46	2.42	19.64
Rosenmuller fossa to petrous ICA	56	11.22	3.00	6.03	17.04
Pharyngeal tubercle of occipital bone to parapharyngeal ICA	56	25.48	3.20	16.71	31.64
Anterior tubercle of atlas to the parapharyngeal ICA	56	22.82	3.69	15.20	27.94
MPP to parapharyngeal ICA at Rosenmuller fossa	56	26.06	3.30	15.15	31.83
MPP to parapharyngeal ICA at basis nasi	56	26.57	4.06	16.05	34.36
LPP to parapharyngeal ICA at Rosenmuller fossa	56	19.70	3.20	14.02	26.06
LPP to parapharyngeal ICA at basis nasi	56	19.71	3.65	11.73	27.23
Length of the Vidian canal	56	14.40	1.93	9.37	19.48
Opening of the Vidian canal to foramen rotundum	56	7.75	2.23	4.45	12.65
Foramen lacerum to external aperture of petrous ICA	56	15.77	1.39	12.62	19.09
Foramen ovale to external aperture of petrous ICA	56	13.51	2.14	8.86	17.98
Foramen spinosum to external aperture of petrous ICA	56	7.49	1.52	3.77	9.98
Sulcus tubae to external aperture of petrous ICA	56	6.19	1.33	3.36	9.33

Abbreviations: ICA, internal carotid artery; LPP, lateral pterygoid plate; Min, minimum; Max, maximum; MPP, medial pterygoid plate; SD, standard deviation.

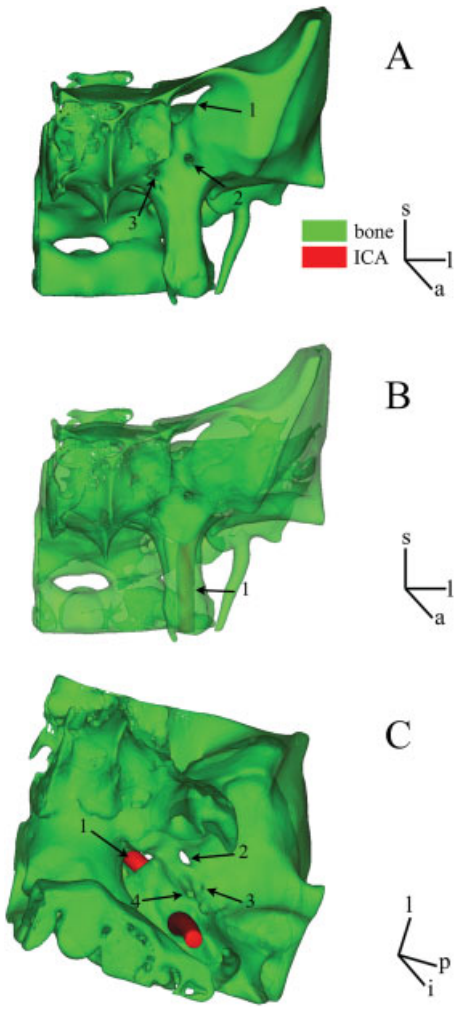

Fig. 2 3D reconstruction of the bone structure around nasopharynx. (A) Anterior view of the sphenoid bone (1, superior orbital fissure; 2, foramen rotundum; 3, the opening of Vidian canal). (B) Parapharyngeal ICA behind the pterygoid process could be identified after the bone was set transparent (1, parapharyngeal ICA). (C) Skull base of the parapharyngeal space from an inferior view (1, foramen lacerum; 2, foramen ovale; 3, foramen spinosum; 4, sulcus tubae). 3D, three-dimension; ICA, internal carotid artery; i, inferior; l, lateral; p, posterior.

reconstructed slices, the distance between the foramen lacerum and the external aperture of petrous ICA was 15.77 ± 1.39 mm; the distance between the foramen ovale and the external aperture of petrous ICA was 13.51 ± 2.14 mm; the distance between the foramen spinosum and the external aperture of petrous ICA was 7.49 ± 1.52 mm; while the distance between the sulcus tubae and the external aperture of petrous ICA was 6.19 ± 1.33 mm (►**Table 1**). No significant difference between different sides has been noticed.

Except for the ICA, the pharyngeal trunk of the ascending pharyngeal artery (APA) was another artery running proximately to the nasopharynx. Though the pharyngeal trunk of APA was difficult to be reconstructed in 3D, it could be clearly identified on the oblique or axis images in 62.5% of our cases (35 in 56 cases) (►**Fig. 4D**). In most of the conditions, the pharyngeal trunk of APA traveled anteriorly and medially to the parapharyngeal ICA, and the incidence rate was 45.7% (16 in 35 cases); the pharyngeal trunk of APA could also run medially, anteriorly, laterally, anterior-laterally or irregularly to the parapharyngeal ICA with incidence rates of 5.7, 14.3, 5.7, 5.7, and 22.9%, respectively (2, 5, 2, 2, and 8 in 35 cases, respectively).

Discussion

Endonasal endoscopic approaches can avoid external incisions and craniofacial osteotomy, thus reducing the potential morbidity and shortening the recovery period; while provide excellent illumination and image magnification of the surgical field; therefore is especially suitable for handling areas difficult to access through open approaches. With the continued improvement of endoscopic instruments and surgical skill, otorhinolaryngologists have already extended their practice to the nasopharynx and its surrounding space. In 2005, Yoshizaki first reported endoscopic nasopharyngectomy to treat four patients with rT2 NPC and one patient with sinonasal malignant melanoma.[12] In 2007 and 2009, Chen et al[13] and Chen et al[14] reported another two series of endoscopic nasopharyngectomy to treat residual and recurrent NPC. According to these reports, adequate intranasal exposure of the nasopharynx can be achieved after resection of the posterior half of the nasal septum; and with this method, all rT1 NPC as well as most rT2 NPC could be resected with clear margins.

During these endoscopic procedures, understanding the anatomic relationship between the landmarks of nasopharyngeal cavity and ICA is critical for a safe and accurate surgical orientation. In the present study, by investigating the 3D and multiplanar reconstructed CTA images of nasopharynx, we found the fossa of Rosenmuller usually just point to the parapharyngeal ICA in the horizontal direction; and in most cases, the deepest place of Rosenmuller fossa is the nearest point of the whole nasopharyngeal cavity to both parapharyngeal and petrous ICA. In this study, we also qualified several other anatomic relationships between bony landmarks of the nasopharyngeal cavity to the parapharyngeal ICA. Though our study is based on Chinese people and racial variance could not be avoided, the quantitative data of our study may still facilitate the surgeon to establish a safe endoscopic dissection in the nasopharynx.

APA usually arises from the posterior wall of external carotid artery, after a short common trunk, it divides into two major branches: the pharyngeal trunk which distributed in the lateral wall of pharynx; and the neuromeningeal trunk which enters the posterior fossa through the foramen magnum.[21,22] In our study, we found the pharyngeal trunk of APA could be identified on the axis or multiplanar reconstructed image of CTA in most cases; and it usually lies anteriorly and medially to the parapharyngeal ICA. This indicates the pharyngeal trunk of APA can be used as an important landmark to locate the parapharyngeal ICA when dissecting in the nasopharynx. For the pharyngeal trunk of APA is the main feeder

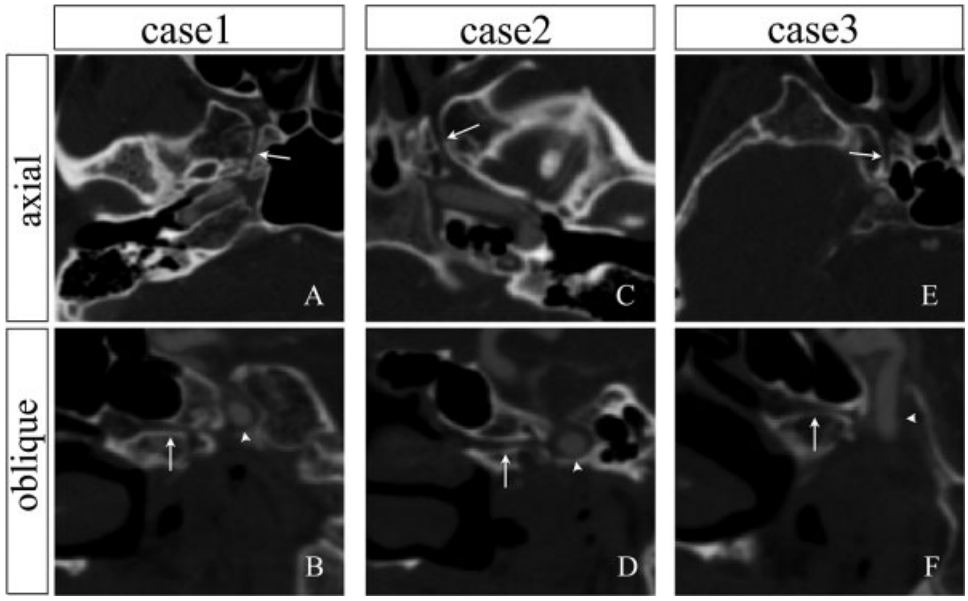

Fig. 3 The anatomic relationship between the Vidian canal and petrous ICA on CTA images. The arrow indicates Vidian canal in all the panels. (A) Axial images of case1 patient. (B) Oblique slice of case1 patient showing the opening of the Vidian canal in the middle cranial fossa is below the horizontal segment of petrous ICA. The arrowhead indicates the horizontal segment of petrous ICA. (C) Axial images of case 2 patient. (D) Oblique slice of case 2 patient showing the opening of Vidian canal in the middle cranial fossa is just pointing to the horizontal segment of petrous ICA. The arrowhead indicates the horizontal segment of petrous ICA. (E) Axial images of case 3 patient. (F) Oblique slice of case 2 patient showing the opening of Vidian canal in the middle cranial fossa is pointing to the anterior vertical segment of petrous ICA and above the level of horizontal segment of petrous ICA. The arrowhead indicates the anterior vertical segment of petrous ICA. CTA, computed tomography angiography; ICA, internal carotid artery.

of nasopharyngeal wall; in theory, selective embolization of it can significantly reduce the blood loss during endoscopic nasopharyngectomy, though such a management may prolong the time of wound healing.

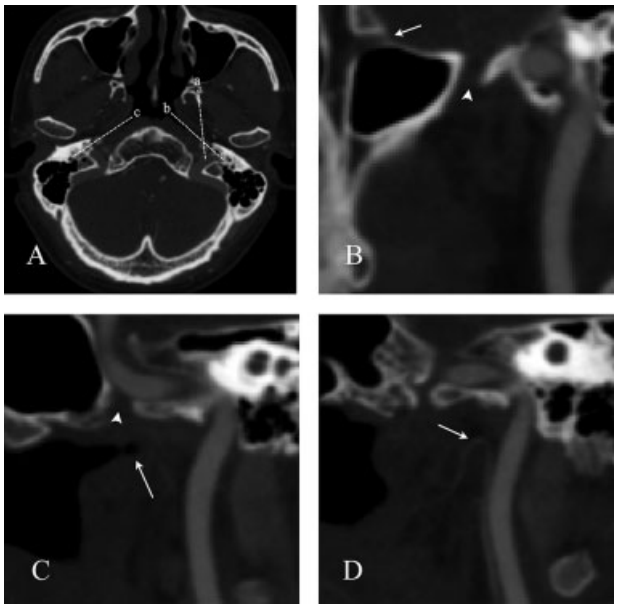

Fig. 4 Multiplanar reconstructed CTA images. (A) Axial image showing the projection of different multiplanar reconstructed images. (B) Slice through line a. Arrow indicates the foramen rotundum, arrowhead indicates the foramen ovale. (C) Slice through line b. Arrow indicates the fossa of Rosenmuller, arrowhead indicates the foramen lacerum. (D) Slice through line c. Arrow indicates the pharyngeal trunk of APA. APA, ascending pharyngeal artery; CTA, computed tomography angiography.

Malignancy originated from the nasopharynx can also infiltrates into its neighboring spaces. Lateral or posterior-lateral into the infratemporal fossa is the most common direction of spread for NPC.[23,24] It has also been reported skull base erosion is detected in up to one-third of NPC patients.[25] To obtain a complete resection of the diffused lesion, otorhinolaryngologist has already extended their endoscopic practice into the surrounding region of nasopharynx. Castelnuovo et al reported a modified medial maxillectomy followed by drilling of the medial pterygoid plate to expose the parapharyngeal space near nasopharynx.[17] Al-Sheibani et al described a similar approach which can control the parapharyngeal and petrous ICA, thus guarantees the tumor to be safely resected by removal of the pterygoid process and the cartilaginous Eustachian tube.[18] When performing the above endoscopic dissections in the infratemporal fossa, the medial pterygoid plate, lateral pterygoid plate, foramen lacerum, foramen ovale, foramen spinosum, and sulcus tubae are important bony landmarks to identify the parapharyngeal ICA. In a cadaveric analysis, Wen et al[26] reported the distance from the posterior margin of lateral pterygoid plate to the parapharyngeal ICA was 19.48 $\pm$ 1.24 mm which correlates well with our result. But they reported a lesser distance from the posterior margin of medial pterygoid plate to the parapharyngeal ICA (20.09 $\pm$ 1.57 mm) compared with our study. They also reported a greater distance from the foramen lacerum to the carotid foramen (19.32 $\pm$ 1.40 mm) compared with our study. In another cadaveric study, Paullus et al reported the foramen spinosum and foramen ovale laid an average of 4.7 (range, 2.5–8.0 mm) and 4.4 mm (range, 2.0–9.0 mm) to the

carotid canal, respectively[27]; these distances were significantly shorter comparing with our results.

As mentioned in previous literatures, Vidian canal is an important landmark to expose petrous ICA in endonasal endoscopic approach.[28,29] The length of it just indicates the distance from the posterior wall of the pterygopalatine fossa to the petrous ICA. In our study, the length of the Vidian canal was 14.40 $\pm$ 1.93 mm which is a bit shorter than the Vescan and colleagues report where the length was around 18 mm.[28] In the current study, we found the opening of Vidian canal in the middle cranial fossa could be either above, below, or just at the level of horizontal segment of petrous ICA; this observation is significantly different from previous reports where the ICA was never located inferior and medial Vidian canal.[28,29] Our result indicates there is still possible risk to circumferentially drill along Vidian canal from an inferior direction to expose the petrous ICA. We also found Vidian canal runs mainly in a medial to lateral direction with a percentage of 94.8%. This result correlates well with the report of Vescan et al where the percentage was 97.7% on the right side and 93.2% on the left side.[29] Though it has been reported that the Vidian canal could run in a lateral to medial pattern,[30] we did not find such a condition in our research.

Reconstructed CTA is not only a potent tool in anatomic study; it can also help the surgeon to obtain individual anatomic information preoperatively. However, this technique still has its own shortcomings. It is difficult to clearly identify soft tissues in CTA image; yet some soft tissues, such as the longus capitis, the cartilaginous portions of the Eustachian tube, the posteromedial trunk of V3 and the stylopharyngeal aponeurosis were important landmarks to locate ICA.[26,31] So this technique should be used combining with magnetic resonance imaging to obtain a careful and complete preoperative assessment.

Acknowledgments

We thank other members of our research group for their helpful discussion. This work was supported by grant no. 81271084 from National Natural Science Foundation of China and grant no. 11411952300 from Biomedical Innovation Plan of Shanghai Committee of Science and Technology.

References

1 Chong VF, Fan YF, Mukherji SK. Carcinoma of the nasopharynx. Semin Ultrasound CT MR 1998;19(6):449–462
2 Marcus KJ, Tishler RB. Head and neck carcinomas across the age spectrum: epidemiology, therapy, and late effects. Semin Radiat Oncol 2010;20(1):52–57
3 Yu MC, Yuan JM. Epidemiology of nasopharyngeal carcinoma. Semin Cancer Biol 2002;12(6):421–429
4 Leung TW, Tung SY, Sze WK, et al. Treatment results of 1070 patients with nasopharyngeal carcinoma: an analysis of survival and failure patterns. Head Neck 2005;27(7):555–565
5 Ong YK, Solares CA, Lee S, Snyderman CH, Fernandez-Miranda J, Gardner PA. Endoscopic nasopharyngectomy and its role in managing locally recurrent nasopharyngeal carcinoma. Otolaryngol Clin North Am 2011;44(5):1141–1154
6 Hao SP, Tsang NM. Surgical management of recurrent nasopharyngeal carcinoma. Chang Gung Med J 2010;33(4):361–369
7 Fisch U. The infratemporal fossa approach for nasopharyngeal tumors. Laryngoscope 1983;93(1):36–44
8 Wei WI, Lam KH, Sham JS. New approach to the nasopharynx: the maxillary swing approach. Head Neck 1991;13(3):200–207
9 Fee WE Jr, Gilmer PA, Goffinet DR. Surgical management of recurrent nasopharyngeal carcinoma after radiation failure at the primary site. Laryngoscope 1988;98(11):1220–1226
10 Tu GY, Hu YH, Xu GZ, Ye M. Salvage surgery for nasopharyngeal carcinoma. Arch Otolaryngol Head Neck Surg 1988;114(3): 328–329
11 Morton RP, Liavaag PG, McLean M, Freeman JL. Transcervico-mandibulo-palatal approach for surgical salvage of recurrent nasopharyngeal cancer. Head Neck 1996;18(4):352–358
12 Yoshizaki T, Wakisaka N, Murono S, Shimizu Y, Furukawa M. Endoscopic nasopharyngectomy for patients with recurrent nasopharyngeal carcinoma at the primary site. Laryngoscope 2005; 115:1517–1519
13 Chen MK, Lai JC, Chang CC, Liu MT. Minimally invasive endoscopic nasopharyngectomy in the treatment of recurrent T1-2a nasopharyngeal carcinoma. Laryngoscope 2007;117(5):894–896
14 Chen MY, Wen WP, Guo X, et al. Endoscopic nasopharyngectomy for locally recurrent nasopharyngeal carcinoma. Laryngoscope 2009;119(3):516–522
15 Ko JY, Wang CP, Ting LL, Yang TL, Tan CT. Endoscopic nasopharyngectomy with potassium-titanyl-phosphate (KTP) laser for early locally recurrent nasopharyngeal carcinoma. Head Neck 2009; 31(10):1309–1315
16 Rohaizam J, Subramaniam SK, Vikneswaran T, Tan VE, Tan TY. Endoscopic nasopharyngectomy: the Sarawak experience. Med J Malaysia 2009;64(3):213–215
17 Castelnuovo P, Dallan I, Bignami M, et al. Nasopharyngeal endoscopic resection in the management of selected malignancies: ten-year experience. Rhinology 2010;48(1):84–89
18 Al-Sheibani S, Zanation AM, Carrau RL, et al. Endoscopic endonasal transpterygoid nasopharyngectomy. Laryngoscope 2011;121(10): 2081–2089
19 Shu CH, Cheng H, Lirng JF, et al. Salvage surgery for recurrent nasopharyngeal carcinoma. Laryngoscope 2000;110(9):1483–1488
20 Zhen G, Fang-lu C, Pei-dong D. The anatomic relationship around the horizontal segment of petrous internal carotid artery: a study based on reconstructed computed tomography angiography. Surg Radiol Anat 2012;34(8):695–700
21 Lasjaunias P, Moret J. The ascending pharyngeal artery: normal and pathological radioanatomy. Neuroradiology 1976;11(2):77–82
22 Hacein-Bey L, Daniels DL, Ulmer JL, et al. The ascending pharyngeal artery: branches, anastomoses, and clinical significance. AJNR Am J Neuroradiol 2002;23(7):1246–1256
23 Chong VFH. Masticator space in nasopharyngeal carcinoma. Ann Otol Rhinol Laryngol 1997;106(11):979–982
24 Chong VFH, Fan YF. Pictorial review: radiology of the carotid space. Clin Radiol 1996;51(11):762–768
25 Chong VFH, Fan YF, Khoo JBK. Nasopharyngeal carcinoma with intracranial spread: CT and MR characteristics. J Comput Assist Tomogr 1996;20(4):563–569
26 Wen YH, Wen WP, Chen HX, Li J, Zeng YH, Xu G. Endoscopic nasopharyngectomy for salvage in nasopharyngeal carcinoma: a novel anatomic orientation. Laryngoscope 2010;120(7):1298–1302
27 Paullus WS, Pait TG, Rhoton AI Jr. Microsurgical exposure of the petrous portion of the carotid artery. J Neurosurg 1977;47(5): 713–726
28 Kassam AB, Vescan AD, Carrau RL, et al. Expanded endonasal approach: vidian canal as a landmark to the petrous internal carotid artery. J Neurosurg 2008;108(1):177–183

29 Vescan AD, Snyderman CH, Carrau RL, et al. Vidian canal: analysis and relationship to the internal carotid artery. Laryngoscope 2007; 117(8):1338–1342
30 Kim HS, Kim DI, Chung IH. High-resolution CT of the pterygopalatine fossa and its communications. Neuroradiology 1996;38 (Suppl 1):S120–S126
31 Falcon RT, Rivera-Serrano CM, Miranda JF, et al. Endoscopic endonasal dissection of the infratemporal fossa: Anatomic relationships and importance of eustachian tube in the endoscopic skull base surgery. Laryngoscope 2011;121(1):31–41